Understanding Bond Formation in Polar One-Step Reactions. Topological Analyses of the Reaction between Nitrones and Lithium Ynolates

David Roca-López,[†] Victor Polo,[‡] Tomás Tejero,[†] and Pedro Merino*,[†]

[†]Laboratorio de Síntesis Asimétrica, Departamento de Síntesis y Estructura de Biomoléculas, Instituto de Síntesis Química y Catálisis Homogénea (ISQCH), Universidad de Zaragoza, CSIC, Campus San Francisco, E-50009 Zaragoza, Aragón, Spain

[‡]Departamento de Química Física and Insitituto de Biocomputación y Física de Sistemas Complejos (BIFI), Universidad de Zaragoza, Campus San Francisco, E-50009 Zaragoza, Aragón, Spain

Ⓢ Supporting Information

ABSTRACT: The mechanism of the reaction between nitrones and lithium ynolates has been studied using DFT methods at the M06-2X/cc-pVTZ/PCM=THF level. After the formation of a starting complex an without energy barrier, in which the lithium atom is coordinated to both nitrone and ynolate, the reaction takes place in one single kinetic step through a single transition structure. However, the formation of C−C and C−O bonds takes place sequentially through a typical *two-stage, one-step process*. A combined study of noncovalent interactions (NCIs) and electron localization functions (ELFs) of selected points along the intrinsic reaction coordinate (IRC) of the reaction confirmed that, in the transition structure, only the C−C bond is being formed to some extent, whereas an electrostatic interaction is present between carbon and oxygen atoms previous to the formation of the C−O bond. Indeed, the formation of the second C−O bond only begins when the first C−C bond is completely formed without formation of any intermediate. Once the C−C bond is formed and before the C−O bond formation starts the RMS gradient norm dips, approaching but not reaching 0, giving rise to a *hidden intermediate*.

An only transition structure but sequential bond formation.
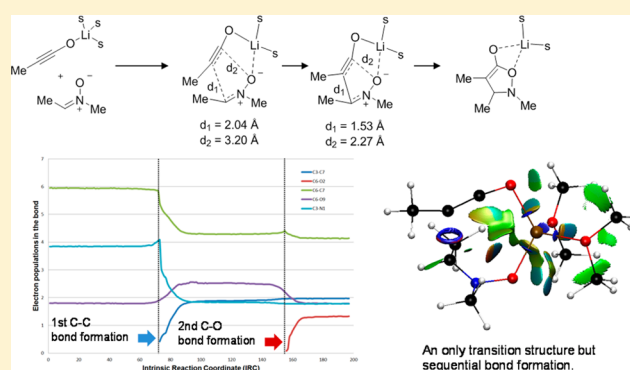
INTRODUCTION

Nitrones **1** have amply demonstrated their synthetic utility in [3 + 2] cycloadditions over the last 75 years.[1] More recently, they have been shown to be excellent electrophiles in nucleophilic additions of organometallic reagents.[2] In this context, we have reported that chiral nonracemic α-alkoxy and α-amino nitrones react with a variety of organometallic reagents, including organolithium[3] and Grignard[4] derivatives, in a completely stereocontrolled way. The stereocontrol is exerted either by using different Lewis acids as precomplexing agents, as in the case of α-alkoxy nitrones,[5] or by selecting the appropriate protecting groups, in the case of α-amino nitrones.[6] In all cases, the first step of the reaction is the formation of complex **2** between the nitrone and the organometallic reagent through coordination of the nitrone oxygen (Scheme 1).[3,7] Such coordination increases the electrophilic character of the azomethine carbon of the nitrone, and for certain cases the complex was proved unequivocally by NMR spectroscopy[7b,8] and X-ray crystallography.[9]

Of particular interest are the reactions of nitrones with species bearing an electron-rich multiple bond such as lithium and silyl ketene acetals[10] and lithium ynolates,[11] leading in all cases to isoxazolidin-2-ones (Scheme 2). We have demon-

Scheme 1. Nucleophilic Addition of Organometallic Reagents to Nitrones


M = Li, MgBr
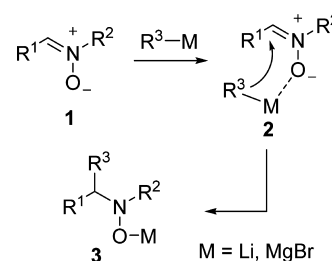
strated that, whereas the reaction with lithium ketene acetals (lithium α-methoxyenolates) takes place through a stepwise mechanism,[10] for the reaction with silyl ketene acetals both one-step and stepwise mechanisms are competitive, although in some cases the stepwise mechanism is prevalent.[12]

On the other hand, much less is known about the mechanism of the reaction between lithium ynolates **5** and nitrones, which has been described[11] as a typical inverse-demand [3 + 2]

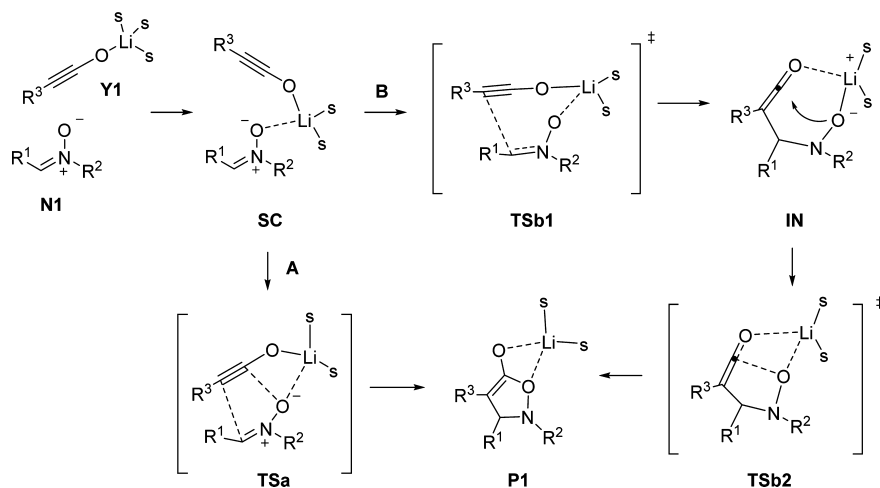**Scheme 2. Addition of Electron-Rich Double Bonds to Nitrones**
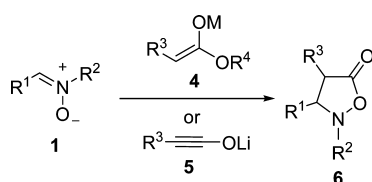
cycloaddition (Scheme 3, route A) by analogy with other similar processes. However, a stepwise mechanism (Scheme 3, route B) involving the sequential formation of the two bonds and the existence of ketene intermediate **IN** could also be considered in a similar way to the reaction of lithium α-alkoxyenolates.

In this work, a density functional theory (DFT) study of the addition of ynolates to nitrones, which has been experimentally studied,[11] has been carried out in order to determine the concertedness of the process and to understand the bond formation. A complete characterization of the electronic reorganization along the reaction is fulfilled by applying topological ELF and NCI analyses of selected points of the IRC.

■ **COMPUTATIONAL METHODS**

All of the calculations were performed using the Gaussian09 program.[13] Molecular geometries were optimized with the M06-2X functional[14] in conjunction with the cc-pVTZ basis set.[15] This method has been recently used in theoretical investigations with nitrones.[16] Analytical second derivatives of the energy were calculated to classify the nature of every stationary point, to determine the harmonic vibrational frequencies, and to provide zero-point vibrational energy corrections. The thermal and entropic contributions to the free energies were also obtained from the vibrational frequency calculations, using the unscaled frequencies. All transition structures were characterized by one imaginary frequency. All of the located TSs were confirmed to connect to reactants and products by intrinsic reaction coordinate (IRC) calculations.[17] The IRC paths were traced using the second-order González–Schlegel integration method.[18] Calculations have been carried out considering solvent effects (THF) with the PCM model[19] and including discrete molecules of dimethyl ether to complete the coordination sphere of lithium.[20] NCI (noncovalent interactions) were computed using the methodology previously described.[21] Data were obtained with the NCIPLOT

program.[21c] A density cutoff of $\rho = 0.1$ au was applied, and the diagrams were created for an isosurface value of $s = 0.4$ and colored in the $[-0.03, 0.03]$ au (sin λ_2)ρ range using VMD software.[22] The electronic structures of stationary points were analyzed by a topological analysis of the electron localization function (ELF).[23] The ELF study was performed with the TopMod program[24] using the corresponding monodeterminantal wave functions of all structures of the IRC. The analysis of the gradient field or topology of ELF[25] has been shown to be a powerful tool for rationalizing the electron delocalization in molecular systems,[26] providing detailed insight of the nature of the chemical bond in a variety of reacting systems.[27] Animation given in the Supporting Information was created by extracting and processing all points of the IRC with an in-house program and saving the corresponding images to create an animated GIF. Nitrone **N1** ($R^1 = R^2 = Me$) and ynolate **Y1a** ($R^3 = Me$) have been chosen as models for the study. In addition, the reaction with the simplest ynolate **Y1b** ($R^3 = H$) has been calculated for the purposes of comparison (Scheme 4).

Scheme 4. Reaction between Nitrone N1 and Ynolates Y1a,b
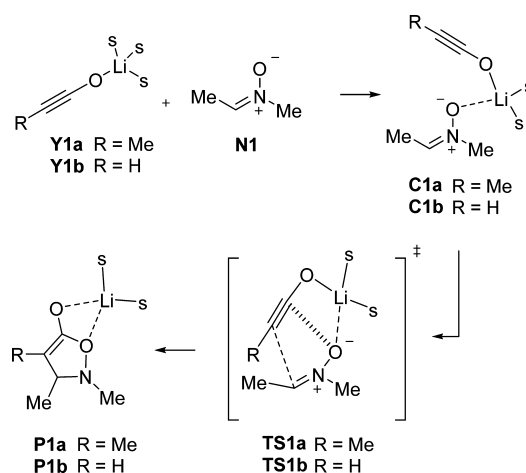
■ **RESULTS AND DISCUSSION**

Addition of Lithium Ynolate. The first step in the reaction between **N1** and **Y1a** is the formation of complex **C1a** without an energy barrier (Scheme 4) in a way similar to the reaction of nitrones with other organolithium reagents.[10] After formation of complex **C1a** only **TS1a** could be located at 9.4

Scheme 3. One-Step (A) and Stepwise (B) Mechanisms for the Reaction between Lithium Ynolates and Nitrones

kcal/mol above the ground state. The geometrical constraints imposed by both the linear triple bond and the coordination to lithium avoids the possibility of considering other approaches between nitrone and ynolate.

The energy profile for the reaction and main geometrical features of **TS1a** and other stationary points are given in Figure 1, while Table 1 reports absolute and relative energies. The C−
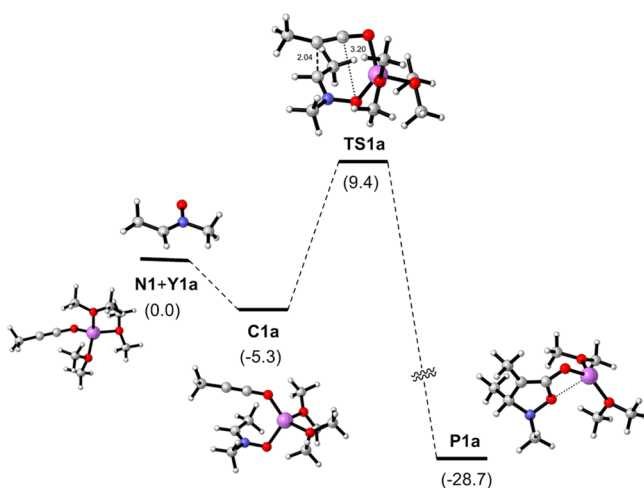

Figure 1. Energy diagram (M06-2X/cc-pVTZ/PCM=THF) and stationary points for the reaction betweeen nitrone **N1** and lithium ynolate **Y1a**. Relative free energy values (ΔG_{298}) are given in kcal/mol.

Table 1. Calculated (M06-2X/cc-pVTZ/PCM=THF) Free (ΔG, hartrees) and Relative Energies ($\Delta\Delta G$, kcal/mol) of the Stationary Points Corresponding to the Reaction of Nitrone N1 with Y1a[a]

	ΔG	$\Delta\Delta G$[b]
N1	−248.34944	
Y1a	−663.73457	
C1a	−757.13530	−5.3
TS1a	−757.11198	9.4
P1a	−757.17258	−28.7

[a]For the nomenclature of the stationary points see Figure 1. [b]Referenced to isolated starting materials (**N1** + **Y1a**); an isolated molecule of the solvent (Me$_2$O) has been added for coherence.

C and C−O distances found in **TS1a** were 2.04 and 3.20 Å, respectively. This computed transition structure corresponds to an apparent one-step but highly asynchronous cycloaddition. However, in contrast to typical dipolar cycloadditions of nitrones,[28] the C−O distance is more in agreement with an electrostatic interaction rather than a forming bond, as reported by Schleyer and co-workers[29] in the case of polar [3 + 2] cycloadditions. Any attempt to locate a ketene intermediate such as **IN** (Scheme 3) failed. We found that structures of this type are not stable as equilibrium states. Attempts to optimize them led back to complex **C1a** (or go ahead to **P1a**), strong evidence that a stepwise mechanism for this reaction is not favored. Similar results have been found with ynolate **Y1b**, which formed the corresponding **C1b** leading to **P1b** through **TS1b** (for geometries, energy data, and details see the Supporting Information) with an energy barrier of 8.1 kcal/mol.

The ultimate reason for the instability of a species such as **IN**, in which the lithium atom is coordinated to the oxygen atoms,

is due to geometrical restrictions imposed by the hybridization of the ynolate carbon atom bonded to the oxygen. The carbon atom which is highly electrophilic does not change the sp hybridization during the first half of the reaction. Consequently, it is too close to the nucleophilic nitrone oxygen and a collapse between the two centers takes place in the second half of the reaction (for an animation see the Supporting Information). Thus, the formation of **P1a** takes place in a single kinetic step but in two stages. Actually, the formation of the two new σ bonds is nonconcerted and the process can be considered a typical two-stage reaction, in agreement with the definition given by Domingo and co-workers.[30]

The intrinsic reaction coordinate illustrated in Figure 2 confirms the two-stage character of the reaction as well as the presence of a so-called *hidden intermediate*.[31] The IRC analysis (Figure 2) also explains the difference in C−C and C−O forming bond lengths observed in **TS1a**. Monitoring of the two forming bonds is also illustrated in Figure 2. Initially (first stage), at **TS1a**, the C−C bond is forming ($d_{C−C}$ = 2.04 Å), whereas the C−O distance ($d_{C−O}$ = 3.20 Å) only indicates a noncovalent interaction (see below) but not a bond formation. After this TS is passed and the reaction progresses (point **a**), the C−C bond is practically formed ($d_{C−C}$ = 1.56 Å), whereas the C−O bond is still not formed ($d_{C−O}$ = 2.86 Å) and the IRC slope is relaxed. In the middle of the formed plateau the hidden intermediate is revealed (point **b**, $d_{C−C}$ = 1.54 Å, $d_{C−O}$ = 2.63 Å). At the end of the plateau (point **c**), the C−C bond is already formed ($d_{C−C}$ = 1.53 Å) and the C−O bond is being formed ($d_{C−O}$ = 2.27 Å). Only at the end of the reaction (point **d**) could the C−O bond be considered formed ($d_{C−O}$ = 1.44 Å). A close inspection of the RMS gradient norm along the IRC reveals that whereas for **TS1** the norm is 0.00 (as expected for a transition structure), at point b (*hidden intermediate*) the norm dips, approaching but not reaching 0.

Rzepa and co-workers pointed out that hidden intermediates could be evidenced as real species by electronically influencing the corresponding geometry.[32] However, in our case, the sp hybridization of the ynolate carbon linked to oxygen forces a collapse between that carbon and nitrone oxygen once the first C−C bond is formed. We tried to reveal a real intermediate by adding an additional discrete solvent molecule in order to affect the geometry of the TS and thus increase the distance between the carbon and oxygen atoms. In fact, under such conditions it was possible to identify the corresponding minimum **IN1a** at 3.9 kcal/mol above the reagents (**N1** and **Y1a**) (Scheme 5). The O−Li and C−O distances were found to be 2.88 and 3.10 Å, respectively. The existence of intermediate **IN1a** could account for an alternative stepwise mechanism in which the lithium atom maintains a pentacoordinated environment. However, the corresponding species bearing pentacoordinated lithium were less stable, in agreement with previous calculations.[33] The corresponding starting complex **C2a** is located 3.9 kcal/mol above the reagents, and the TS **TS2a**, leading to **IN1**, has an energy barrier of 15.2 kcal/mol (5.8 kcal/mol higher in energy than the Li-tetracoordinated **TS1a**). Consequently, the possibility of a stepwise mechanism should be disregarded. The elimination of the terminal methyl group at the ynolate (**Y1b**) does not affect the results and a similar pathway that was higher in energy than the corresponding Li-tetracoordinated pathway was found (for geometries, energy data, and details see the Supporting Information).

NCI and ELF Analyses. To understand the C−C and C−O bond formation processes along the *two-stage, one-step* addition
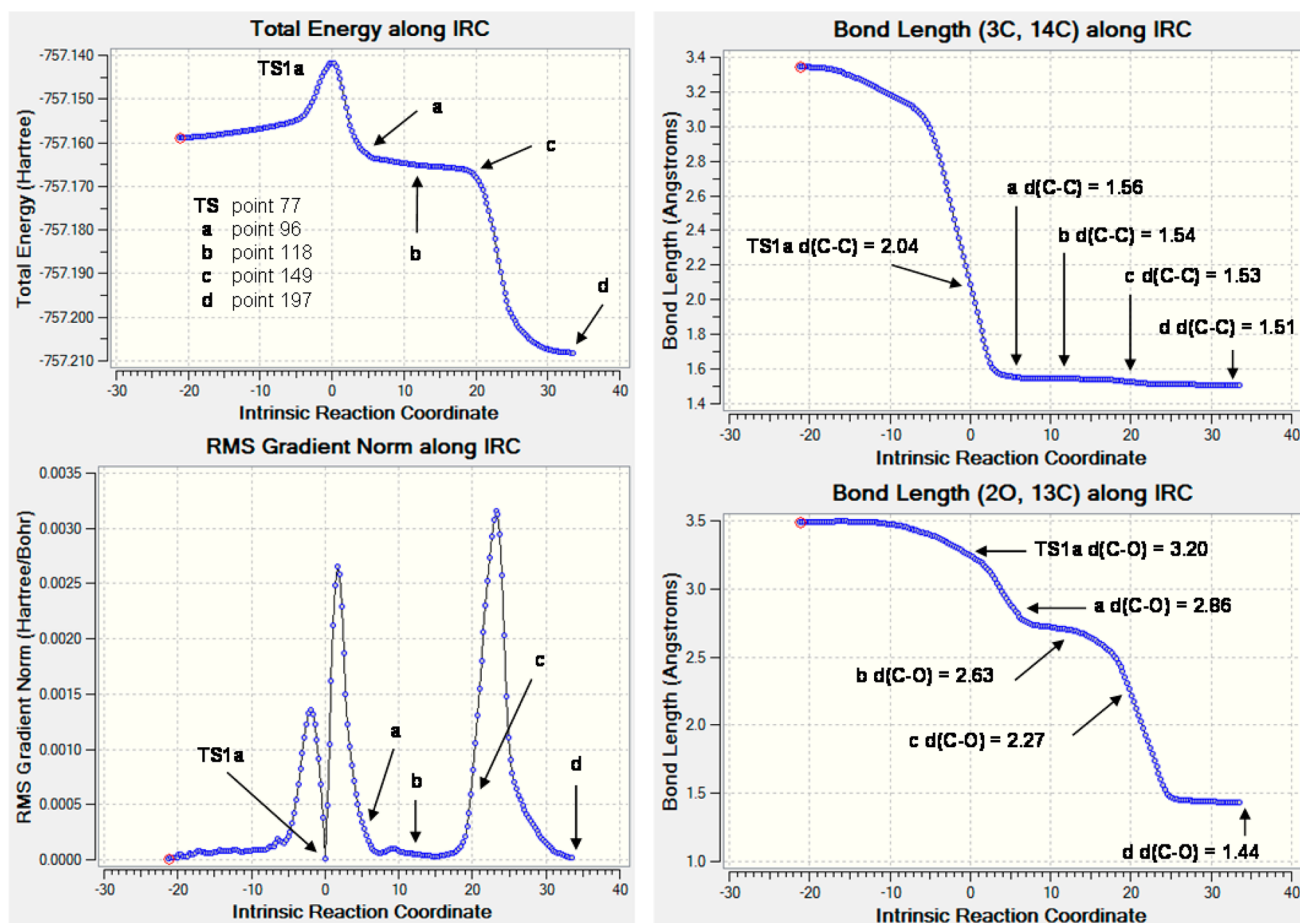
Figure 2. Computed (M06-2X/cc-pVTZ/PCM=THF) intrinsic reaction coordinate (IRC) for the reaction between nitrone **N1** and ynolate **Y1a**, showing the relative energy (top left), the gradient norm showing a prominent hidden intermediate (bottom left), and monitoring of C−C (top right) and C−O (bottom right) bonds along the IRC. Selected points of the IRC are **TS1a**, **a**, **b**, **c**, and **d**.

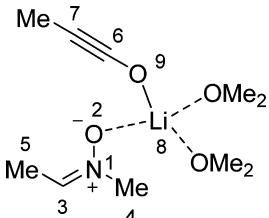## Scheme 5. Reaction between N1 and Y1a,b with Pentacoordinated Lithium[a]
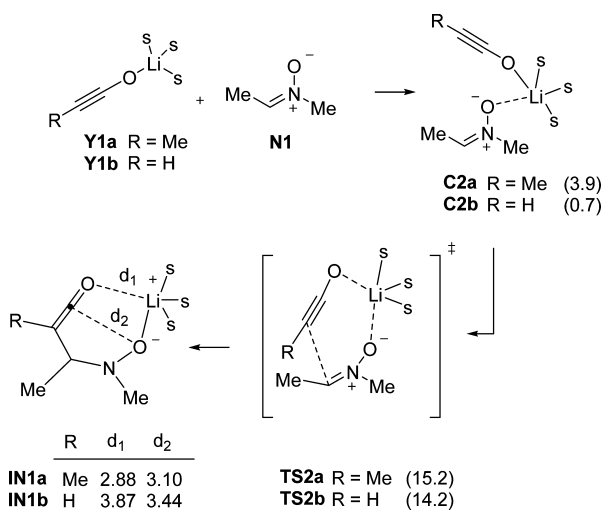
[a]Relative energies to reagents (**N1** + **Y1a** or **N1** + **Yb**) calculated at the M06-2X/cc-pVTZ/PCM=THF level are given in parentheses.

of lithium ynolates to nitrones, topological ELF and NCI analyses of selected relevant points of the IRC have been carried out. ELF analysis has been revealed as an excellent tool to understand bonding changes along the reaction path.[34]

Domingo and co-workers reported several examples illustrating the utility of this topological analysis.[35] NCI analysis[20a,21] shares several similarities with the atoms in molecules approach but, in addition, three-dimensional regions are provided in order to detect, in a qualitative way, both attractive (van der Waals and hydrogen bonding) and repulsive (steric) interactions.[36] The NCI analysis, which only requires the density function, $\rho(r)$, has been demonstrated to be efficient and applicable to a variety of systems,[37] including nucleophilic additions to C=N double bonds.[38] We carried out the complete ELF analysis for the IRC (197 points) illustrated in Figure 2 for the reaction between nitrone **N1** and ynolate **Y1a**. From this analysis we considered points 77 (**TS1**), 79, 80, 158, and 159 of the IRC as the most relevant ones according to Domingo and co-workers, who showed that single-bond formation between two atoms begins by merging two monosynaptic basins into a new disynaptic basin, associated with the formation of the new bond.[39] The ELF basin populations of those selected points, including initial complex **C1a** and final product **P1a**, are given in Table 2. The attractor positions and the atom numbering of ELF and NCI for relevant points of the IRC are shown in Figure 3.

The ELF topological analysis of the attractors for starting complex **C1a** shows three disynaptic basins each associated with the C−C triple bond, whose electron density integrates to 5.95 e (e.g., $V_1(C6,C7)$, $V_2(C6,C7)$ and $V_3(C6,C7)$) and with the C=N double bond, whose electron density integrates to

Table 2. ELF Basin Populations for the Reaction of Nitrone N1 with Y1a[a]

	C1a[a]	TS1a[b]	P79	P80	P158	P159	P1a[c]
d(C3–C7)	3.35	2.04	1.98	1.93	1.52	1.51	1.51
d(C6–O2)	3.49	3.20	3.22	3.21	1.79	1.74	1.44
V(C3)			0.10				
V(C7)		0.74	0.94				
V(C3,C7)				1.18	1.97	1.96	1.97
V(C6)					0.19		
V(O2)					0.39		
V(C6,O2)						0.68	1.33
V_1(C6,C7)	2.15	2.51	2.42	2.38	2.10	2.09	2.08
V_2(C6,C7)	1.59	2.06	2.46	2.42	2.18	2.17	2.06
V_3(C6,C7)	2.21						
V_1(C3,N1)	1.86	2.71	2.41	2.33	1.78	1.78	1.78
V_2(C3,N1)	1.98						

[a]Corresponding to the initial point 1 of the IRC. [b]Corresponding to point 77 of the IRC. [c]Corresponding to the final point 197 of the IRC.

3.84 e (e.g., V_1(N1,C3) and V_2(N1,C3)). The picture for the final product **P1a** displays two disynaptic attractors associated with the expected C–C (e.g., V(C3,C7)) and C–O (e.g., V(C6,O2)) new single bonds integrating to 1.97 and 1.33 e, respectively. Also, two disynaptic attractors associated with a C–N single bond (e.g., V(N1,C3)) and C–C double bond (e.g., V_1(C6,C7)) and V_2(C6,C7) integrating to 1.78 and 4.14 e, respectively, are shown. The NCI analysis of **C1a** (Figure 4) shows a clear favorable interaction (green–blue surface) between the π systems corresponding to ynolate and nitrone.

At **TS1a** no monosynaptic basin appears at the nitrone carbon C3, but one is present for the C6 atom integrating to 0.74 e. At this TS the C6–C7 bonding region is characterized by V(C6,C7) integrating to 4.57 e (from 5.95 e at **C1a**), indicating that transfer of the electron density from the triple bond to the nitrone has started. Indeed, the C3–N1 bonding region is characterized by only one disynaptic basin V(C3,N1) integrating to 2.71 e (from 3.84 e at **C1a**). The NCI analysis of **TS1a** shows the forming bond as a strong favorable interaction (blue ring) corresponding to the electronic transference mentioned above. In addition, a weak interaction (green surface) is present between the nitrone oxygen and C6. This observation is in agreement with a favorable interaction but not with a forming bond between C6 and O2 atoms. At **P79**, the V(C7) monosynaptic basin increases to 0.94 e and a new monosynaptic basin V(C3) integrating to 0.1 e appears at the electrophilic center C3 of the nitrone moiety. These monosynaptic basins merge into a new disynaptic basin, V(C3,C7) integrating to 1.18 e, at the following point of the IRC (**P80**), indicating that the first C3–C7 bond is already being formed at d(C3,C7) = 1.93 Å. The NCI analysis reflects that the same favorable interaction between C6 and O2 observed for **TS1a** is still present (Figure 4), while the C3–C7 bond has been completely formed.

Going ahead on the IRC, the V(C3,C7) disynaptic basin increases its population until 1.86 e at point 97 (point **a**, Figure 2) with a C3–C7 distance of 1.56 Å; at this point the C3–C7 bond is essentially formed. Notably, no monosynaptic basins appear at C6 and O2, indicating that, at this point, the formation of the second C6–O2 single bond has not begun. At **P158**, the C3–C7 bond is formed completely (d(C3,C7) = 1.52 Å) and the electron density of the V(C3,C7) disynaptic basin is 1.97 e. At this point, two new V(C6) and V(O2) monosynaptic basins appear, integrating to 0.19 and 0.39 e, respectively. At **P159** (d(C3,C7) = 1.51 Å, d(C6,O2) = 1.74 Å), these monosynaptic basins merge into the new V(C6,O2) disynaptic basin integrating to 0.68 e, which corresponds with
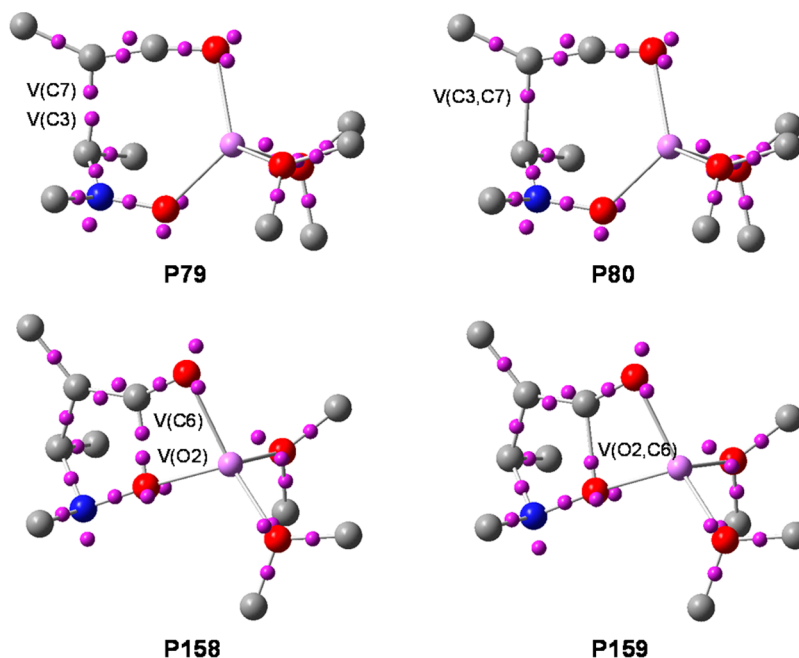

P79

P80

P158

P159

Figure 3. Most relevant ELF attractors at selected points of the IRC of the reaction between nitrone **N1** and ynolate **Y1a**.

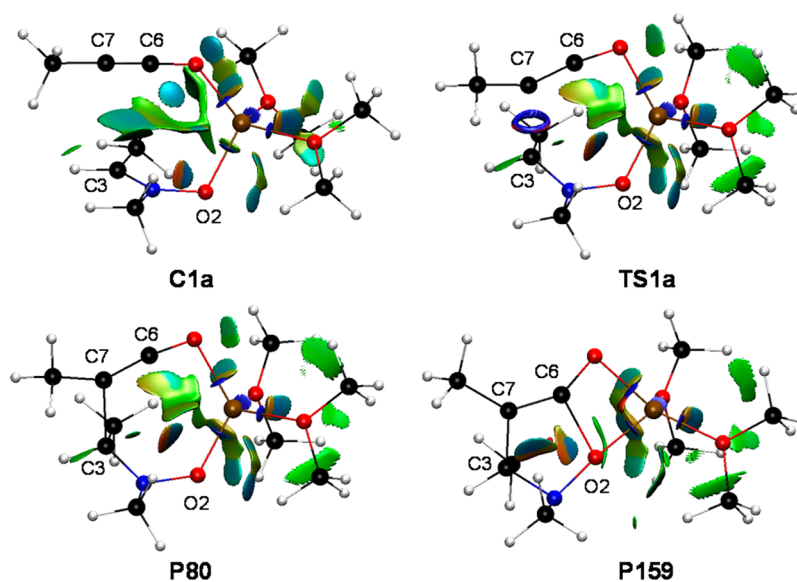**Figure 4.** NCI analysis of relevant points **C1a**, **TS1a**, **P80**, and **P159**.
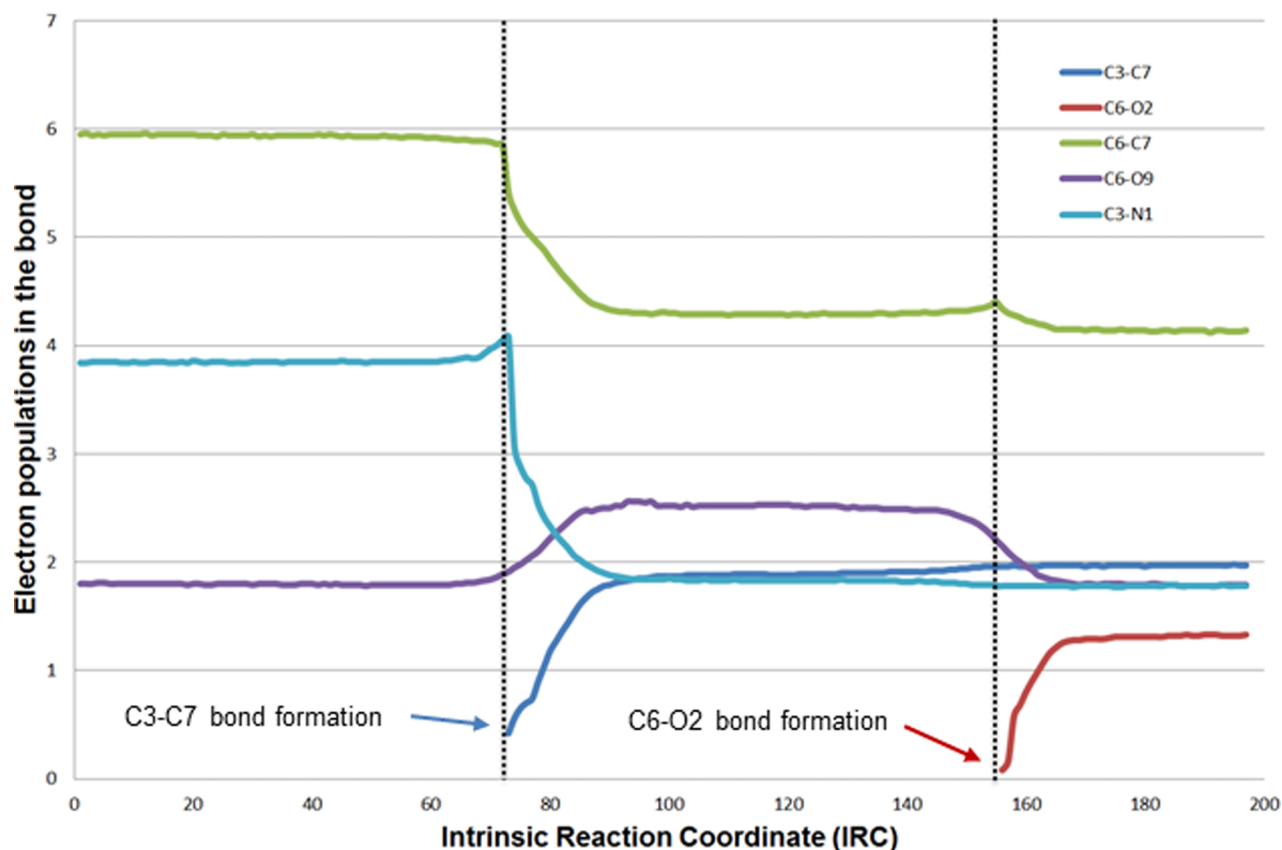

Figure 5. Evolution of electronic basin populations along the reaction coordinate. An EP value close to 6 represents a triple bond, while those close to 4 and 2 represent double and single bonds, respectively.

the formation of the second C6−O2 single bond. The NCI analysis of **P159** (Figure 4) also reflects a transformation of the previously observed favorable interaction into the bond between C6 and O2 atoms (for a complete animation of both ELF and NCI analyses for the whole IRC see the Supporting Information).

These results are in agreement with a *two-stage, one step* process in which, initially, the C3−C7 single bond is formed in

the first part of the reaction path, whereas the second C6−O2 single bond is formed during the second part of the reaction. Figure 5 shows the evolution of electronic populations along the reaction coordinate for selected bonds. When the first C3−C7 bond is formed, the C3−N1 double bond becomes a single bond and, simultaneously, the C6−C7 triple bond becomes a double bond. At the same time the C6−O9 bond increases its population up to 2.6 e, too low to be considered a double bond.

Consequently, it is evident that a species resembling a ketenic intermediate is not formed at any moment. This situation is maintained along the reaction until the second C6−O2 bond is formed. At that moment, the electronic population of the C6−O9 bond returns to typical values corresponding to a single bond. The bond-forming evolution illustrated in Figure 5 is fully consistent with a chemical reaction accounting of a single kinetic step, as it is evident that the two bonds C3−C7 and C6−O2 are formed in a consecutive way.

CONCLUSIONS

In summary, in the reaction of nitrones with ynolates both sp hybridization and coordination to the lithium atom are responsible for placing carbon and oxygen atoms at such a distance in **TS1** which, given the electronic and geometric features of the reaction, results in close enough contact to promote the formation of the C−O bond once the C−C bond is formed in a typical two-stage reaction corresponding to a single kinetic step. Consequently, no ketene intermediates are formed. The ELF bonding analysis of the IRC of the reaction confirms the highly asynchronous mechanism in which the formation of C−C and C−O bonds of the final isoxazolidine accounts in a consecutive way. Transfer of electronic density from the triple bond of the ynolate toward the electrophilic C−N double bond is completed during the first stage of the reaction, and only when the first C−C bond is formed does the formation of the second C−O bond begin. The NCI analysis is consistent with the presence of favorable interactions between C6 and O2 prior to the bond formation and reveals the moment in which the new bonds are formed.

ASSOCIATED CONTENT

Ⓢ Supporting Information

Figures, tables, and files giving details of calculations corresponding to the reaction of unsubstituted ynolate **Y1b** and to the reaction of **Y1a** and **Y1b** through lithium pentacoordinated species at the M06-2X/cc-pVTZ/PCM=THF level of theory, Cartesian coordinates of optimized structures, animated graphics (GIF and MOV format) illustrating the progress of the reaction, NCI and ELF analysis, and evolution of ELF descriptors along the reaction coordinate. This material is available free of charge via the Internet at http://pubs.acs.org.

AUTHOR INFORMATION

Corresponding Author

*E-mail for P.M.: pmerino@unizar.es.

Notes

The authors declare no competing financial interest.

ACKNOWLEDGMENTS

REFERENCES

(1) (a) Irvin, L. *Chem. Rev.* **1938**, *23*, 193−285. (b) Hamer, J.; Macaluso, A. *Chem. Rev.* **1964**, *64*, 473−495. (c) Confalone, P. N.; Huie, E. M. *Org. React. (N.Y.)* **1988**, *36*, 1. (d) Martin, J. N.; Jones, R. C. F. Synthetic Applications of 1,3-Dipolar Cycloaddition Chemistry: Nitrones. In *Synthetic Applications of 1,3-Dipolar Cycloaddition Chemistry toward Heterocycles and Natural Products*; Padwa, A., Pearson, W. H., Eds.; Wiley: Chichester, United Kingdom, 2002; Vol. *59*, pp 1−81. (e) Merino, P. Nitrones and Cyclic Analogues. In *Compounds with Two Carbon−Heteroatom Bonds: Heteroatom Analogues of Aldehydes and Ketones*; Pawda, A., Bellus, D., Eds. Georg Thieme Verlag: Stuttgart, New York, 2004; Vol. *27*, pp 511−580. (f) Merino, P. *Science of Synthesis, Knowledge Updates* **2011**, 325−404.
(2) (a) Merino, P. *Compt. Rend. Chim.* **2005**, *8*, 775−788. (c) Lombardo, M.; Trombini, C. *Curr. Org. Chem.* **2002**, *6*, 695−713. (d) Lombardo, M.; Trombini, C. *Synthesis* **2000**, 759−774.
(3) Merino, P.; Revuelta, J.; Tejero, T.; Cicchi, S.; Goti, A. *Eur. J. Org. Chem.* **2004**, 776−782.
(4) Delso, I.; Tejero, T.; Goti, A.; Merino, P. *J. Org. Chem.* **2011**, *76*, 4139−4143.
(5) Merino, P.; Jimenez, P.; Tejero, T. *J. Org. Chem.* **2006**, *71*, 4685−4688.
(6) Merino, P.; Lanaspa, A.; Merchan, F. L.; Tejero, T. *Tetrahedron: Asymmetry* **1997**, *8*, 2381−2401.
(7) Delso, I.; Marca, E.; Mannucci, V.; Tejero, T.; Goti, A.; Merino, P. *Chem. - Eur. J.* **2010**, *16*, 9910−9919.
(8) Chiacchio, U.; Rescifina, A.; Saita, M. G.; Iannazzo, D.; Romeo, G.; Mates, J. A.; Tejero, T.; Merino, P. *J. Org. Chem.* **2005**, *70*, 8991−9001.
(9) Carmona, D.; Lamata, M. P.; Viguri, F.; Rodriguez, R.; Oro, L. A.; Lahoz, F. J.; Balana, A. I.; Tejero, T.; Merino, P. *J. Am. Chem. Soc.* **2005**, *127*, 13386−13398.
(10) Merino, P.; Tejero, T. *Synlett* **2011**, 1967−1977 and references cited therein.
(11) (a) Shindo, M.; Ohtsuki, K.; Shishido, K. *Tetrahedron: Asymmetry* **2005**, *16*, 2821−2831. (b) Shindo, M.; Itoh, K.; Ohtsuki, K.; Tsuchiya, C.; Shishido, K. *Synthesis* **2003**, 1441−1445. (c) Shindo, M.; Ohtsuki, K.; Shishido, K. *Org. Lett.* **2002**, *4*, 3119−3121.
(12) Domingo, L. R.; Arno, M.; Merino, P.; Tejero, T. *Eur. J. Org. Chem.* **2006**, 3464−3472.
(13) Frisch, M. J.; Trucks, G. W.; Schlegel, H. B.; Scuseria, G. E.; Robb, M. A.; Cheeseman, J. R.; Scalmani, G.; Barone, V.; Mennucci, B.; Petersson, G. A.; Nakatsuji, H.; Caricato, M.; Li, X.; Hratchian, H. P.; Izmaylov, A. F.; Bloino, J.; Zheng, G.; Sonnenberg, J. L.; Hada, M.; Ehara, M.; Toyota, K.; Fukuda, R.; Hasegawa, J.; Ishida, M.; Nakajima, T.; Honda, Y.; Kitao, O.; Nakai, H.; Vreven, T.; Montgomery, J. A., Jr.; Peralta, J. E.; Ogliaro, F.; Bearpark, M.; Heyd, J. J.; Brothers, E.; Kudin, K. N.; Staroverov, V. N.; Kobayashi, R.; Normand, J.; Raghavachari, K.; Rendell, A.; Burant, J. C.; Iyengar, S. S.; Tomasi, J.; Cossi, M.; Rega, N.; Millam, J. M.; Klene, M.; Knox, J. E.; Cross, J. B.; Bakken, V.; Adamo, C.; Jaramillo, J.; Gomperts, R.; Stratmann, R. E.; Yazyev, O.; Austin, A. J.; Cammi, R.; Pomelli, C.; Ochterski, J. W.; Martin, R. L.; Morokuma, K.; Zakrzewski, V. G.; Voth, G. A.; Salvador, P.; Dannenberg, J. J.; Dapprich, S.; Daniels, A. D.; Farkas, Ö.; Foresman, J. B.; Ortiz, J. V.; Cioslowski, J.; Fox, D. J. *Gaussian 09. Revision D1*; Gaussian, Inc., Wallingford, CT, 2009.
(14) Zhao, Y.; Truhlar, D. G. *Acc. Chem. Res.* **2008**, *41*, 157−167.
(15) (a) Dunning, T. H., Jr. *J. Chem. Phys.* **1989**, *90*, 1007−1023. (b) Kendall, R. A.; Dunning, T. H., Jr.; Harris, R. J. *J. Chem. Phys.* **1992**, *96*, 6796−6806. (c) Woon, D. E.; Dunning, T. H., Jr. *J. Chem. Phys.* **1993**, *98*, 1358−1371.
(16) Roca-López, D.; Tejero, T.; Merino, P. *J. Org. Chem.* **2014**, *79*, 8358−8365.
(17) (a) Fukui, K. *J. Phys. Chem.* **1970**, *74*, 4161−4163. (b) Fukui, K. *Acc. Chem. Res.* **1981**, *14*, 363−368.
(18) (a) González, C.; Schlegel, H. B. *J. Phys. Chem.* **1990**, *94*, 5523−5527. (b) González, C.; Schlegel, H. B. *J. Chem. Phys.* **1991**, *95*, 5853−5860.

(19) (a) Barone, V.; Cossi, M.; Tomasi, J. *J. Comput. Chem.* **1998**, *19*, 404−417. (b) Cances, E.; Mennucci, B.; Tomasi, J. *J. Chem. Phys.* **1997**, *107*, 3032−3041. (c) Cossi, M.; Barone, V.; Cammi, R.; Tomasi, J. *Chem. Phys. Lett.* **1996**, *255*, 327−335. (d) Cossi, M.; Scalmani, G.; Rega, N.; Barone, V. *J. Chem. Phys.* **2002**, *117*, 43−54. (e) Tomasi, J.; Persico, M. *Chem. Rev.* **1994**, *94*, 2027−2094.

(20) (a) Domingo, L. R.; Gil, S.; Mestres, R.; Picher, M. T. *Tetrahedron* **1995**, *51*, 7207−7214. (b) Domingo, L. R.; Gil, S.; Mestres, R.; Picher, M. T. *Tetrahedron* **1996**, *52*, 11105−11112.

(21) (a) Johnson, E. R.; Keinan, S.; Mori-Sanchez, P.; Contreras-Garcia, J.; Cohen, A. J.; Yang, W. *J. Am. Chem. Soc.* **2010**, *132*, 6498−6506. (b) Lane, J. R.; Contreras-Garcia, J.; Piquemal, J.-P.; Miller, B. J.; Kjaergaard, H. G. *J. Chem. Theory. Comput.* **2013**, *9*, 3263−3266. (c) Contreras-Garcia, J.; Johnson, E. R.; Keinan, S.; Chaudret, R.; Piquemal, J.-P.; Beratan, D. N.; Yang, W. *J. Chem. Theory. Comput.* **2011**, *7*, 625−632.

(22) Humphrey, W.; Dalke, A.; Schulten, K. *J. Mol. Graph.* **1996**, *14*, 33−38.

(23) (a) Savin, A.; Becke, A. D.; Flad, J.; Nesper, R.; Preuss, H.; Vonschnering, H. G. *Angew. Chem., Int. Ed.* **1991**, *30*, 409−412. (b) Savin, A.; Nesper, R.; Wengert, S.; Fassler, T. F. *Angew. Chem., Int. Ed.* **1997**, *36*, 1808−1832.

(24) Noury, S.; Krokidis, X.; Fuster, F.; Silvi, B. *Comput. Chem.* **1999**, *23*, 597−604.

(25) (a) Savin, A.; Silvi, B.; Colonna, F. *Can. J. Chem.* **1996**, *74*, 1088−1096. (b) Silvi, B. *J. Mol. Struct.* **2002**, *614*, 3−10. (c) Silvi, B.; Savin, A. *Nature* **1994**, *371*, 683.

(26) (a) Angyan, J. G.; Loos, M.; Mayer, I. *J. Phys. Chem.* **1994**, *98*, 5244−5248. (b) Fradera, X.; Bader, M. A.; Austen, R. F. W. *J. Phys. Chem. A* **1999**, *103*, 304−314. (c) Ponec, R.; Strnad, M. *Int. J. Quantum Chem.* **1994**, *40*, 43−53. (d) Silvi, B. *Phys. Chem. Chem. Phys.* **2004**, *6*, 256−260.

(27) (a) Bentabed-Ababsa, G.; Derdour, A.; Roisnel, T.; Saez, J. A.; Perez, P.; Chamorro, E.; Domingo, L. R.; Mongin, F. *J. Org. Chem.* **2009**, *74*, 2120−2133. (b) Berski, S.; Andres, J.; Silvi, B.; Domingo, L. R. *J. Phys. Chem. A* **2006**, *110*, 13939−13947. (c) Domingo, L. R.; Chamorro, E.; Perez, P. *J. Org. Chem.* **2008**, *73*, 4615−4624. (d) Domingo, L. R.; Chamorro, E.; Perez, P. *Org. Biomol. Chem.* **2010**, *8*, 5495−5504. (e) Domingo, L. R.; Picher, M. T.; Arroyo, P. *Eur. J. Org. Chem.* **2006**, 2570−2580. (f) Domingo, L. R.; Picher, M. T.; Arroyo, P.; Saez, J. A. *J. Org. Chem.* **2006**, *71*, 9319−9330. (g) Polo, V.; Andres, J.; Berski, S.; Domingo, L. R.; Silvi, B. *J. Phys. Chem. A* **2008**, *112*, 7128−7136. (h) Polo, V.; Domingo, L. R.; Andres, J. *J. Phys. Chem. A* **2005**, *109*, 10438−10444. (i) Polo, V.; Domingo, L. R.; Andres, J. *J. Org. Chem.* **2006**, *71*, 754−762.

(28) (a) Sims, J.; Houk, K. N. *J. Am. Chem. Soc.* **1973**, *95*, 5798. (b) Krenske, E. H.; Agopcam, S.; Aviyente, V.; Houk, K. N.; Johnson, B. A.; Holmes, A. B. *J. Am. Chem. Soc.* **2012**, *134*, 12010−12015.

(29) Neumann, F.; Lambert, C.; Schleyer, P. v. R. *J. Am. Chem. Soc.* **1998**, *120*, 3357−3370.

(30) Domingo, L. R.; Saez, J. A.; Zaragoza, R. J.; Arno, M. *J. Org. Chem.* **2008**, *73*, 8791−8799.

(31) Kraka, E.; Cremer, D. *Acc. Chem. Res.* **2010**, *43*, 591−601.

(32) Armstrong, A.; Boto, R. A.; Dingwall, P.; Contreras-Garcia, J.; Harvey, M. J.; Masona, N. J.; Rzepa, H. S. *Chem. Sci.* **2014**, *4*, 2057−2071.

(33) Hayes, C. J.; Simpkins, N. S. *Org. Biomol. Chem.* **2013**, *11*, 8458−8462.

(34) Contreras-Garcia, J.; Recio, J. M. *Theor. Chim. Acta* **2011**, *128*, 411−4118.

(35) (a) Domingo, L. R.; Chamorro, E.; Perez, P. *Org. Biomol. Chem.* **2010**, *8*, 5495−5504. (b) Domingo, L. R.; Perez, P.; Jose Aurell, M.; Saez, J. A. *Curr. Org. Chem.* **2012**, *16*, 2343−2351. (c) Domingo, L. R.; Perez, P.; Saez, J. A. *Org. Biomol. Chem.* **2012**, *10*, 3841−3851. (d) Domingo, L. R.; Perez, P.; Saez, J. A. *Tetrahedron* **2013**, *69*, 107−114. (e) Domingo, L. R.; Perez, P.; Saez, J. A. *RSC Adv.* **2013**, *3*, 7520−7528. (f) Domingo, L. R.; Saez, J. A.; Arno, M. *RSC Adv.* **2012**, *2*, 7127−7134.

(36) (a) Alonso, M.; Woller, T.; Martin-Martinez, F. J.; Contreras-Garcia, J.; Geerlings, P.; De Proft, F. *Chem.—Eur. J.* **2014**, *20*, 4931−4941. (b) Contreras-Garcia, J.; Yang, W.; Johnson, E. R. *J. Phys. Chem. A* **2011**, *115*, 12983−12990.

(37) (a) Chaudret, R.; Courcy, B. d.; Contreras-Garcia, J.; Gloaguen, E.; Zehnacker-Rentien, A.; Mons, M.; Piquemal, J.-P. *Phys. Chem. Chem. Phys.* **2014**, *16*, 9876−9891. (b) Zong, L.; Ban, X.; Kee, C. W.; Tan, C.-H. *Angew. Chem., Int. Ed.* **2014**, *53*, 11849−11853. (c) Nava, P.; Carissan, Y.; Drujon, J.; Grau, F.; Godeau, J.; Antoniotti, S.; Dunach, E.; Humbel, S. *ChemCatChem* **2014**, *6*, 500−507. (d) Kemppainen, E. K.; Sahoo, G.; Piisola, A.; Hamza, A.; Kotai, B.; Papai, I.; Pihko, P. M. *Chem. - Eur. J.* **2014**, *20*, 5983−5993. (e) Arbour, J. L.; Rzepa, H. S.; Contreras-Garcia, J.; Adrio, L. A.; Barreiro, E. M.; Hii, K. K. *Chem. - Eur. J.* **2012**, *18*, 11317−11324. (f) Nieto Faza, O.; Fernandez, I.; Silva Lopez, C. *Chem. Commun.* **2013**, *49*, 4277−4279. (g) Xue, X.-S.; Li, X.; Yu, A.; Yang, C.; Song, C.; Cheng, J.-P. *J. Am. Chem. Soc.* **2013**, *135*, 7462−7473.

(38) Hennum, M.; Fliegl, H.; Gundersen, L.-L.; Eisenstein, O. *J. Org. Chem.* **2014**, *79*, 2514−2521.

(39) For a concise and clear definition of basins and their chemical interpretation see: Domingo, L. R. *RSC Adv.* **2014**, *4*, 32415−32428.